

Factors affecting beam intensity and quality in synchrocyclotrons

S. Holm

MSC Division, CERN, Geneva, Switzerland

ABSTRACT

Theories for efficiency of capture and focusing at the centre of a synchrocyclotron are discussed and compared with model experiments. Good agreement is found between theory and experiment on the influence of basic parameters on beam intensity. Measured current values indicate that the goal of $10 \mu\text{A}$ can easily be reached in the improved CERN synchrocyclotron. A factor three or four times this value is in fact possible.

The anticipated construction of the central region will permit injection in well-centred orbits. Quality deterioration due to the necessary polarisation of the dee electrode is avoided by means of a similarly polarised anti-dee at the centre. During the first inward phase oscillations a build-up of radial oscillation amplitudes might occur. In our intended dee construction the amplitudes created by the cut-back angles are small.

1. INTRODUCTION

Theoretical analysis of the capture process¹ and of space charge effects during the initial stages of the acceleration²⁻⁴ has shown that an intense beam can be obtained by the application of an increased accelerating voltage and by the adoption of a closed ion source. Median plane calculations⁵⁻⁷ have described the beam behaviour in the region where the dee angle is $<180^\circ$.

In this paper some further calculations will be reported. These concern essentially the median plane motion during the first few phase oscillations, while the ions are in the region where the dee angle is 180° .

The central region model at CERN provides the possibility to get an experimental verification of some of the calculations mentioned above and to study problems related to central region design. The main data for this small synchrocyclotron is given in Table 1. Maximum proton energy is $\sim 15 \text{ MeV}$ which is sufficient to permit the particles to perform several phase oscillations before reaching final radius. Thus the essential phenomena such as capture of particles into stable acceleration and space charge losses as well as quality determining effects may be studied. The broad band system used to drive the dee⁸ permits an independent variation of voltage, frequency-time derivative and repetition rate by means of programming at low voltage level.⁹

Measurements have so far been performed using central geometries with rf-extraction from the source. The first geometry (referred to as Geometry 1a) consisted simply of a puller with a 3 mm slit placed in front of the ion source chimney at a distance of ~ 2.5 mm from the arc slit (Fig. 1). The puller was offset at an angle of 20° to the gap mid-line in order to increase the initial phase angles, for a gain in capture time as well as electric focusing. The dee and dummy dee near the source consisted of plates giving an acceleration gap of 11 mm in the

Table 1. CERN MODEL CYCLOTRON (MICRO SC) DATA

Pole diam.	84 cm
Pole gap	20 cm
Azimuthally symmetric magnetic field	
Nominal centre field value	19.4 kG
Radial field shape $0 < r \leq 28$ cm	$K = 2$
Dee voltage	≤ 30 kV
Duty cycle	$\leq 5\%$
Broad band system: band width	1 MHz
Useful radius	≈ 30 cm

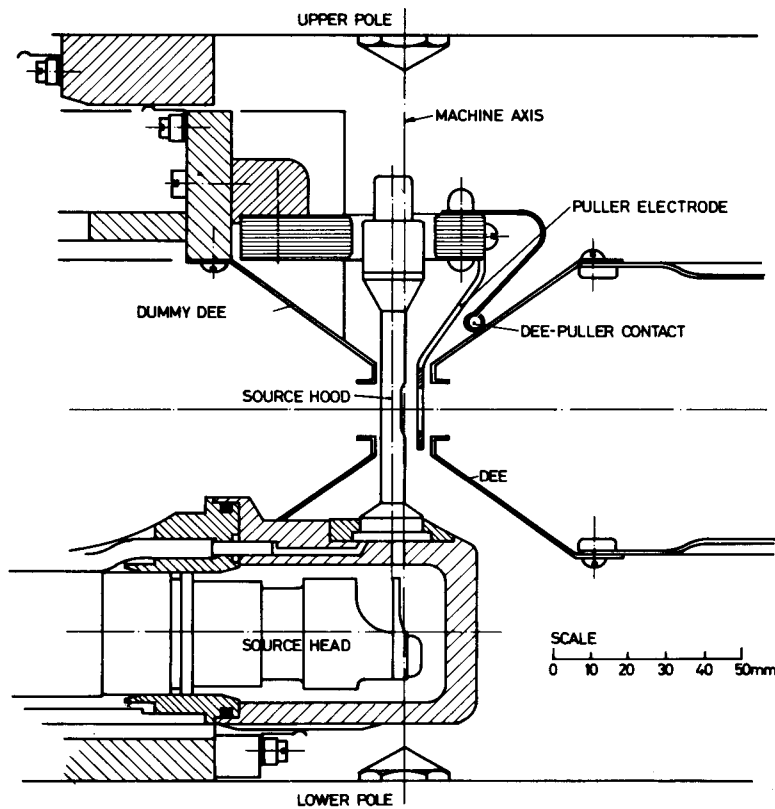


Fig. 1. Central region configuration in the model cyclotron. Geometries 1a and 1b

centre. The half aperture was 7 mm within a radius of 12 mm, thereafter increasing with an angle of 9° . The same geometrical configuration in the median plane was also used together with another set of plates (Geometry 1b) giving a vertical aperture angle to the median plane of 23° . A slightly more refined geometry (Geometry 3) is shown in section in Fig. 2 and in Fig. 3 of reference 10. The two electrodes penetrating the median plane serve here to confine the electric field in order to gain in source clearance on the first turn. The required precise alignment of the electrodes is obtained by mounting the central parts of the dee and dummy dee together, with insulators.

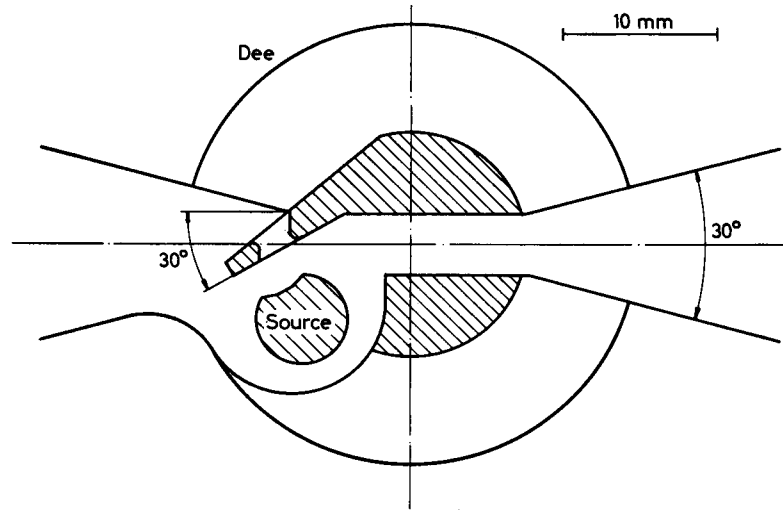


Fig. 2. 25 kV rf extraction geometry (Geometry 3)

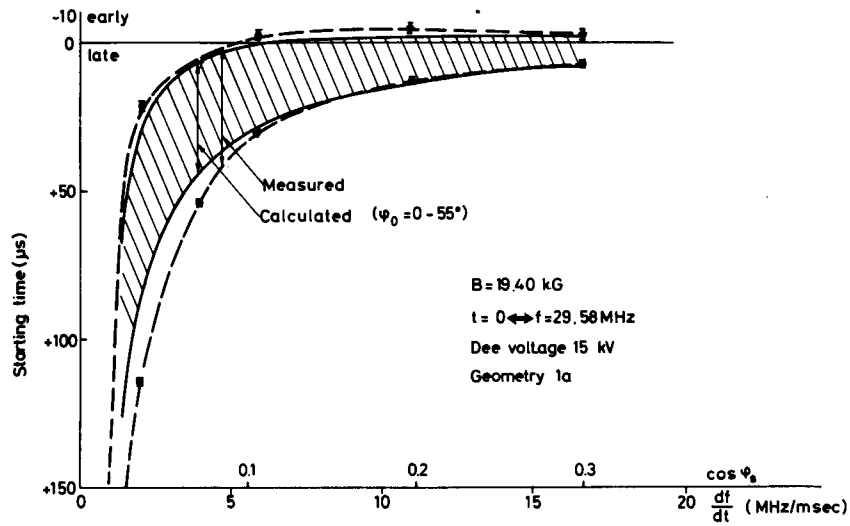


Fig. 3. Region of capture into stable acceleration as function of $\cos \varphi_s$

2. BEAM INTENSITY

2.1. Capture time

An expression for the capture time is given by Kullander:¹

$$\Delta t(\varphi_o, \varphi_s) = \frac{4}{\omega} \left(\frac{\pi E_o}{eVK} \right)^{1/2} \times L(\varphi_o, \varphi_s) / \cos \varphi_s \quad (1)$$

where E_o is the rest energy of the particle, ω is the angular frequency, eV is the maximum energy gain per turn, φ_o and φ_s are the starting phase and the equilibrium phase respectively. $\varphi = 0$ when the particle gains maximum energy. K defines the magnetic field shape from $K = -E/\omega \times d\omega/dE$. The function $L(\varphi_o, \varphi_s)$ is given in reference 1 for several different initial phases with $\varphi_o = 0$ corresponding to the case treated in the Bohm and Foldy theory.¹¹ The value of the equilibrium phase depends on the rate of change of frequency through the relation:

$$\frac{df}{dt} = - \frac{eV\omega^2 K}{2\pi E_s} \cos \varphi_s \quad (2)$$

At low values of $\cos \varphi_s$, where the capture time is largely determined by return of particles to the centre, L increases strongly with φ_o . Predictions using Eqn (1) agree well with experimental results as seen in Fig. 3. The measurements were done by displacing a short ion source pulse over the time interval of interest and recording the limits of zero current at full radius in the machine. As the capture time increases, according to the theory, with starting phase, for these values of $\cos \varphi_s$, the measurements yield the capture time for the highest injected phase. For the geometry used here, the maximum phase was found from electrolytic tank studies to be $\sim 55^\circ$. The uncertainties in determining the beginning and the end of the capture were due to the rather slow rise and fall times of the arc current pulse available.

2.2. Captured beam current

A knowledge of how the charge contained in each beam pulse varies with the equilibrium phase is very important since it determines the choice of frequency modulation rate at injection, and thus the whole frequency-time curve under optimal conditions. A function which describes this variation is given in reference 4. It has been derived under the assumption that the charge density for a given starting phase is determined by the minimum focusing force obtained when combining magnetic and first order electric focusing. The striking feature of the function is that it has an optimum for a value of the equilibrium phase, which depends on the injected phase range. The optimum occurs at $\sim \cos \varphi_s = 0.07$ for $\varphi_o = 0-60^\circ$ and is found at still lower $\cos \varphi_s$ if the phase range is further extended.

In Fig. 4 is shown the measured variation of the total proton beam current with $\cos \varphi_s$ at a fixed repetition rate. The target radius was 25 cm. The calculated space charge limit was $0.41 \mu\text{A}$ at the optimum point, for a dee voltage of 15 kV. The increase of beam current is essentially linear with dee voltage between 15

and 20 kV. This is also predicted by the theory under the assumption that the injected phase range remains constant and that the available aperture for the beam is independent of the dee voltage. The first requirement is roughly fulfilled with this geometry at dee voltages of 15–20 kV. At 10 kV, however, only a part of the phase range gets enough energy to clear the source and extractor at the first turn. The second requirement is approximately fulfilled as the aperture changes little with radius.

Measurements on Geometry 1b gave the result $0.63 \mu\text{A}$ and $0.98 \mu\text{A}$ at the optimum with 15 and 20 kV dee voltage respectively. The increase is thus more rapid than linear. Some preliminary measurements have also been performed on Geometry 3. Due to a larger set back angle of the source and puller (30°) and a more confined electric field¹² the maximum phase angle is theoretically $\sim 70^\circ$. The strictly conical shape of the dee and dummy dee electrodes (at 30° to the median plane) provide an electric field which is essentially directed along the orbits, thus preventing any phase grouping effect. The optimum beam current was found to be $2.0 \mu\text{A}$ at a dee voltage of 25 kV and an rf repetition rate of 50 Hz. The frequency modulation was 6 MHz/ms corresponding to $\cos \varphi_s \approx 0.07$. At $\cos \varphi_s = 0.11$ the current was $1.9 \mu\text{A}$. Scaling these results to the CERN SC parameters gives a beam current of $>20 \mu\text{A}$.

It should be remarked in this connection that the shortest acceleration time compatible with an acceleration without loss of particles out of the stable synchrotron phase space depends on both the magnetic field shape and on the initial value of $\cos \varphi_s$. In the CERN SC the optimised acceleration time decreases relatively slowly with increasing $\cos \varphi_s$ at values around 0.1. The optimum $\cos \varphi_s$ at capture will therefore be only slightly above what is found for constant repetition rate. For the CERN machine the initial $\cos \varphi_s$ has been chosen to be 0.13.

In a semi-isochronous machine, on the other hand, the optimised acceleration time will vary much more rapidly with the initial $\cos \varphi_s$, which therefore has to be chosen much higher in order to optimise the beam current. Also from beam quality point of view a more rapid initial acceleration might be necessary in this case.

3. PHASE WIDTH

Phase width measurements on Geometry 3 using a beam intercepting phase probe have yielded a width of $\sim 100^\circ$ on the first turn. Part of these phases are lost vertically after a few turns. Measurements at fixed frequency of the time distribution of prompt γ -rays from an aluminium target at 15 cm, which was the smallest useful radius with this method, have revealed a phase width of $\sim 40^\circ$. This reduction in phase width is larger than expected, but may be partly explained by radial losses observed between 8 cm and 12 cm radius. A phase compression due to azimuthal space charge forces¹³ is not excluded but remains to be proved.

4. VERTICAL AMPLITUDES

The total beam height when using this geometry was 20 mm at a radius of 20 cm. Scaling to full radius in the CERN SC this yields vertical amplitudes of <6.5 mm corresponding to a vertical emittance of 6π mm mrad. A further increase in

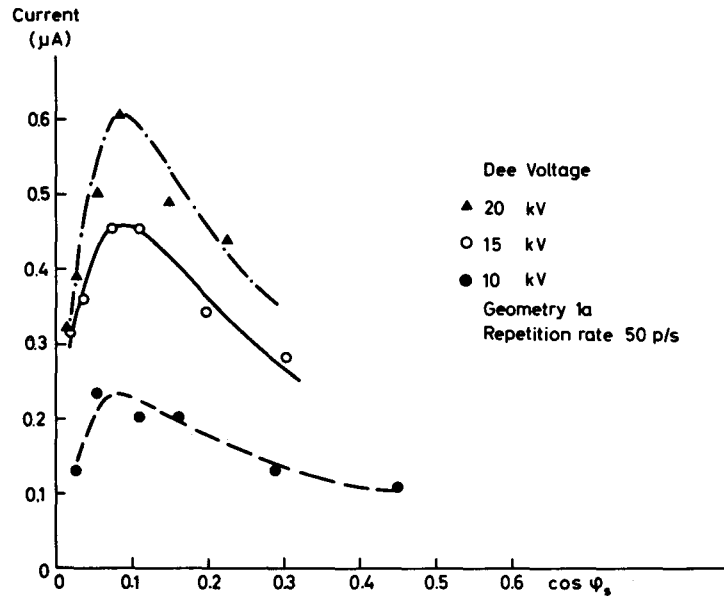


Fig. 4. Measured beam intensity as function of $\cos \varphi_s$

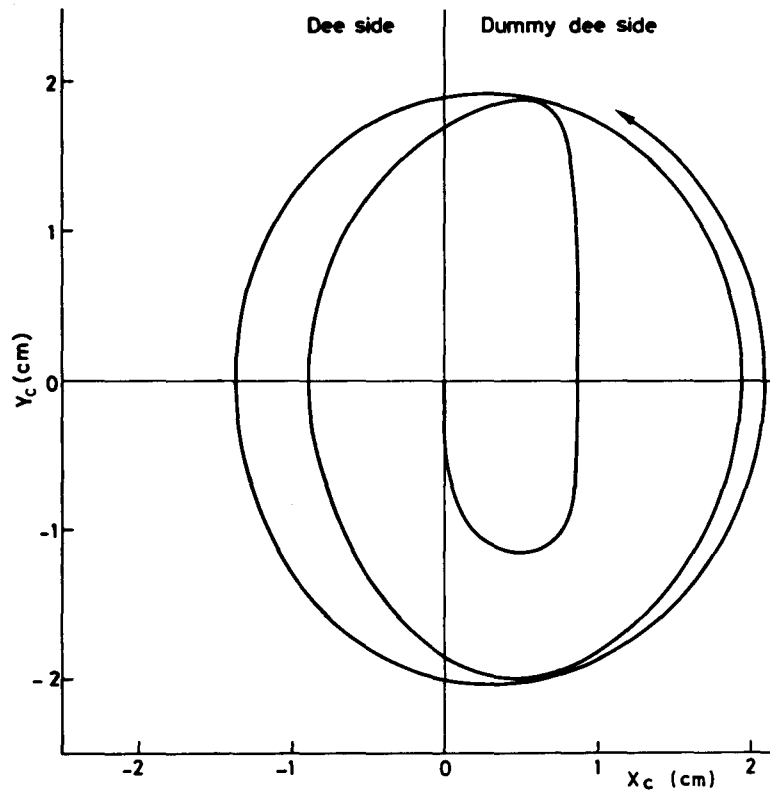


Fig. 5. Motion of orbit centre in presence of dee bias. Rf dee voltage 25 kV. Dee bias -2 kV. Starting time $t_0 = 1 \mu\text{s}$. Initial phase $\varphi_0 = 60^\circ$

intensity can be obtained at the expense of vertical quality by increasing the vertical angle of the cones at the centre. Although the energy gain per turn decreases due to longer gap transit times, an increase in beam current of approximately 70% could be expected with 45° cones. Experiments in the central region model are however limited to 30° due to lack of vertical space.

5. RADIAL AMPLITUDES

The use of a hooded ion source and a narrow acceleration gap configuration permits the initial orbits to be well centred. For the rf geometry shown in Fig. 2, computations show that the initial orbit centre including the spread due to the source emittance, should lie within a circle of 1.5-2 mm radius. Calculations have revealed that a serious increase in radial amplitudes can occur due to cut-back angles of the dee.⁵⁻⁷ For the CERN SC a straight dee gap will therefore be preserved out to a radius of 60 cm and the cut-back angle thereafter increased in steps of 15° . The radial oscillation amplitudes thus created amount to <1 mm.

In order to see whether the initially small amplitudes were preserved in the straight gap region, a computer study has been made of the median plane motion during the first phase oscillations performed by the particles. For this study 'Programme 49' made by Dr. Vogt-Nilsen at CERN has been mainly used. This programme integrates the particle motion in a given magnetic field with acceleration by one or several narrow gaps. The magnetic field shape of the model cyclotron was used in the computations.

A possible source of increased amplitudes is the d.c. bias on the dee, used in order to avoid multipactoring effects. This bias causes an unbalanced energy gain which moves the orbit centre parallel to the dee gap. Assuming $\nu_r \neq 1$ the orbit centre tends to move on a circle with a radius of approximately

$$\rho = \frac{e\Delta V r}{2\pi T \nu_r^2 (1 - \nu_r)} \quad (3)$$

where r = orbit radius
 ΔV = dee bias
 T = kinetic energy.

At small radii where ν_r is near unity, ρ may attain values of a few centimetres. In accelerated motion near the centre the parameters in this expression vary rapidly and the exact motion must be computed. Fig. 5 shows the computed centre movement in a case where a bias of -2 kV and an rf voltage of 25 kV were used. df/dt was -9.14 MHz/ms corresponding to $\cos \varphi_s = 0.1$. The particle was started on centre with an energy of 100 keV and followed during 800 turns. Starting time $t_o = 1 \mu s$, $t_o = 0$ corresponding to resonance condition in the centre and the initial phase angle was $\varphi_o = 60^\circ$. As the final position of the orbit centre depends on φ_o as well as t_o it is not possible to arrive at a centring of all particles. A way of avoiding this effect is to use a small anti-dee at the centre, biased to the same d.c. potential as the dee. For the CERN SC it is planned to extend the biased anti-dee to a radius of 40 cm. The remaining effect of the dee bias and the radial electric field from the anti-dee will create a negligible amplitude of ~ 0.3 mm.¹⁴

Another phenomenon, which might give rise to increased amplitudes near the

centre occurs if an orbit is not centred with respect to the acceleration gap. The particle will then experience a difference in energy gain from one gap crossing to the next due to the difference in time spent between successive crossings. Assuming a narrow, straight gap this results at phase angles near 90° in a drift per turn which is approximately

$$\frac{dy_c}{dn} = \frac{eV}{2T} \sin \varphi \times x_c \quad (4)$$

where x_c and y_c are co-ordinates across and along the gap respectively. eV is the maximum energy gain per turn. T is the kinetic energy and φ is the mean phase angle. The drift is for $v_r < 1$, as is the case for the CERN SC, directed in the same sense as the precession.

The possibility for a build-up of amplitudes due to this effect is present when

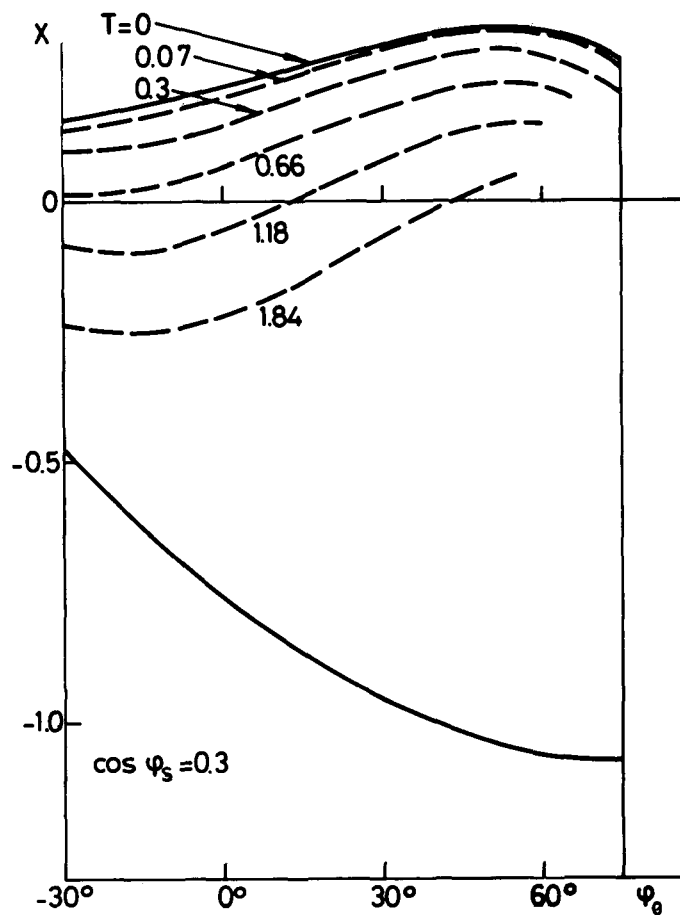


Fig. 6. Capture region. Dashed lines mark starting conditions giving different energies in first radial phase oscillation minimum calculated for $V = 60 \text{ kV}$ and $K = 2$. Horizontal axis is starting phase, φ_0 , vertical axis is initial $d\varphi/dt$ in reduced units

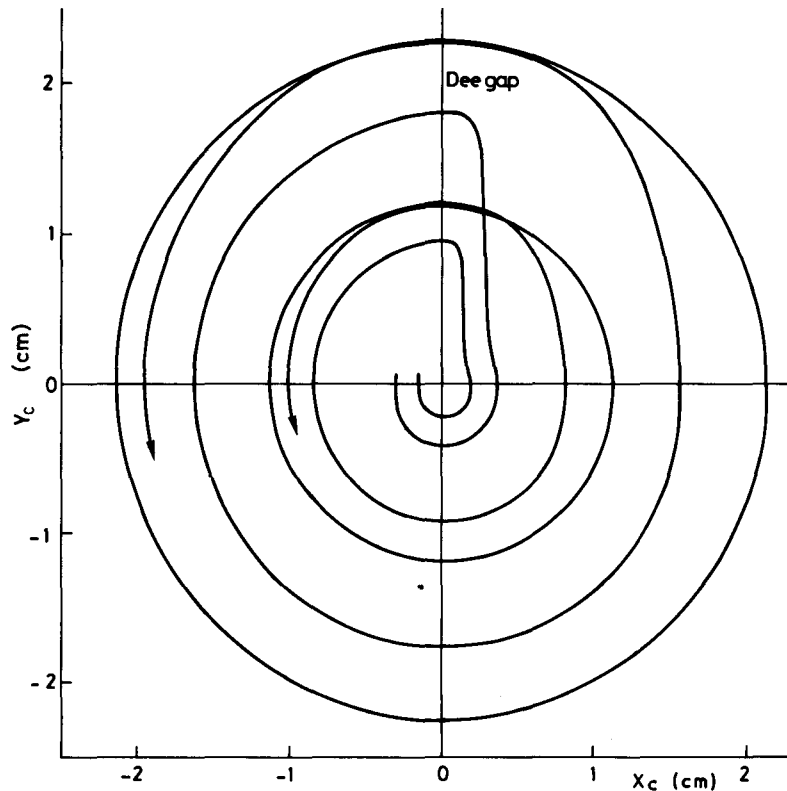


Fig. 7. Motion of orbit centres during the initial 800 turns. Narrow acceleration gap. Dee voltage 25kV. Starting time $t_0 = 7 \mu s$. Initial phase angle $\varphi_0 = 30^\circ$. Initial kinetic energy 103.5 keV

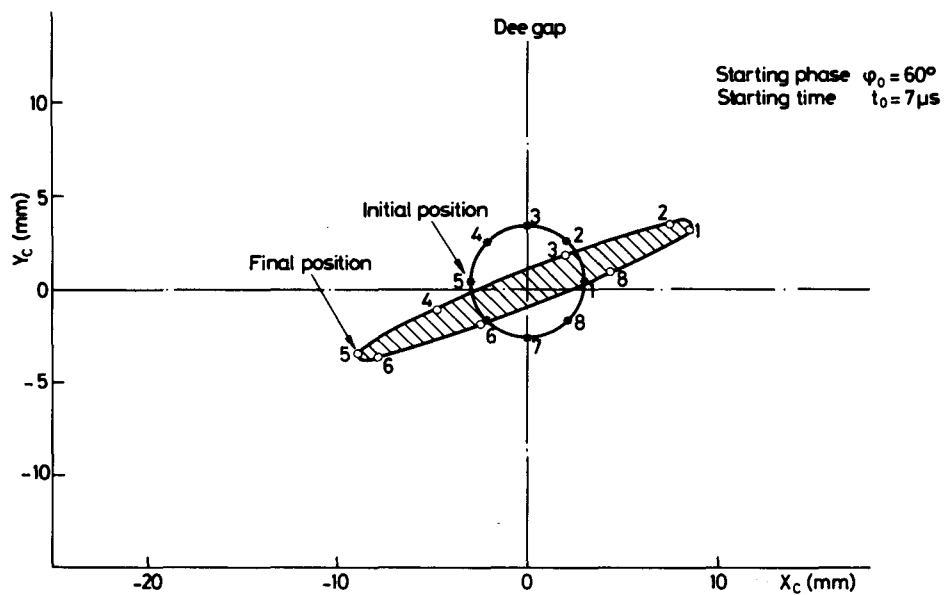


Fig. 8. Distribution of orbit centres. Initial position of eight particles marked with stars. Position after 800 turns of acceleration marked with rings. Dee voltage 25 kV

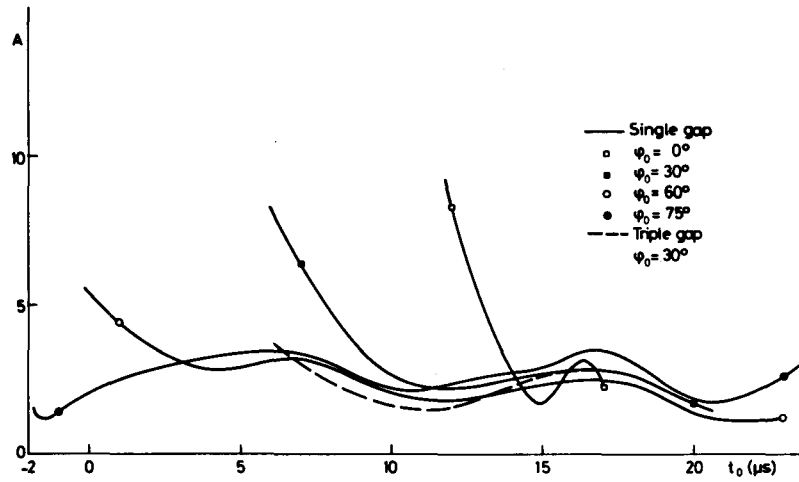


Fig. 9. Blow-up factor as function of starting time at $\cos \varphi_s = 0.1$

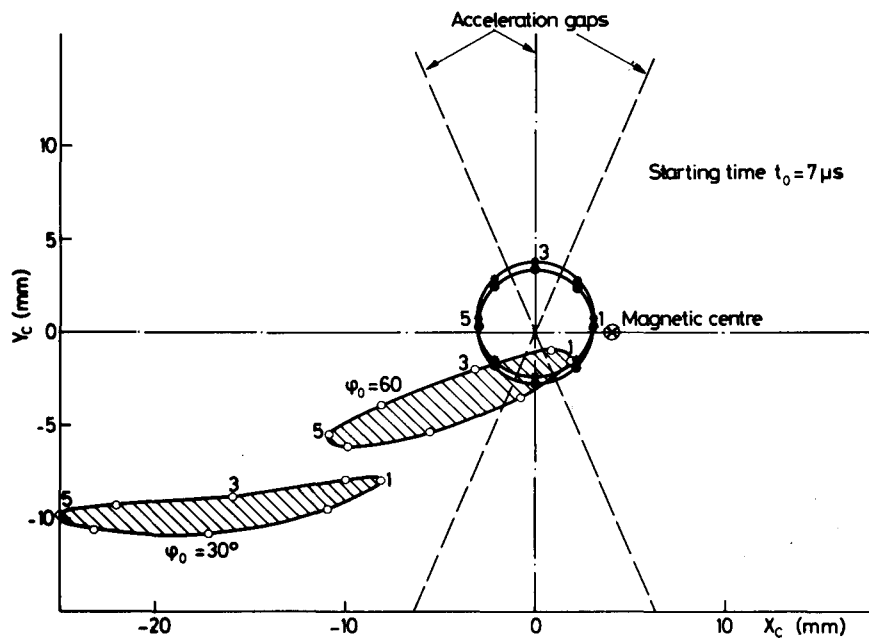


Fig. 10. Distribution of orbit centres after 800 turns when magnetic centre displaced 4 mm. Initial positions marked with stars ($\varphi_0 = 30^\circ$) and dots ($\varphi_0 = 60^\circ$). Acceleration by three gaps, each with an rf voltage of $8\frac{1}{3}$ kV. Angle between the gaps 25°

the particles swing back towards the centre during the first phase oscillation. The minimum energy attained depends on the starting conditions in synchrotron phase space as well as on the rate of increase of the synchronous energy. This is illustrated in Fig. 6 for two values of $\cos \varphi_s$. The vertical axis in the figures gives the starting time through the relation

$$t_o = -\frac{2}{\omega} \times \left(\frac{\pi E_o}{eVK} \right)^{1/2} \times \frac{x}{\cos \varphi_s} \quad (5)$$

where ω is the angular frequency and E_o the rest energy of the particle. $V = 60$ kV and $K = 2$ were used for the calculations. For other values of these parameters the minimum energy follows from

$$T\sqrt{\frac{K}{V}} = \text{const.} \quad (6)$$

From Fig. 6 one can see that the earliest starting particles for a given initial phase will return to the lowest energy. It is also seen that the relative number of particles returning below a certain energy is considerably reduced at a higher $\cos \varphi_s$.

In order to get a quantitative estimate of the amplitude build up by this process a series of computations were made. The motion was followed from an energy slightly above 100 keV for 800 particle turns. The acceleration occurred in a narrow, straight acceleration gap with a voltage of 25 kV. In Fig. 7 is shown the motion of the orbit centres for two particles with initial decentering of 3 and 1.5 mm. Starting time and phase were $7 \mu\text{s}$ and 30° respectively. The displacement parallel to the gap, directed along the y -axis in the figure, occurs when the particle approaches the first radial minimum which in this case was at an energy of 160 keV. A slight displacement is also observed at the second minimum.

Obviously the drift depends strongly on the actual betatron phase, when the particle approaches the minimum radius. Eight initial betatron conditions were therefore used in the runs. These were chosen such that the initial orbit centres were distributed on a circle. Fig. 8 shows the positions of the orbit centres after 800 particle turns in a typical case. Other runs established the linear relation between the major axis M of the final ellipse and the diameter D of the initial circle.

Computer calculations covering the whole range of capture times for four different initial phases have been made for the case $\cos \varphi_s = 0.1$. The result is plotted in Fig. 9 in terms of a 'blow-up factor' $A = M/D$. Full lines mark results using a single narrow acceleration gap. With exception of the case $\varphi_o = 75^\circ$ the earliest starting particles of a given φ_o are thus seen to be subject to the largest blow-up. The slight peaks on the curves are found to occur when the time for returning to the minimum radius is close to the time for one-half or one betatron oscillation.

An ideally narrow gap cannot be realised in practice. In particular when the electrodes in the centre have a conical shape such as is anticipated for the CERN SC, the horizontal electrical field will penetrate into the dee and dummy dee and occupy a horizontal angle approximately equal to twice the angle of the cones to the median plane. In order to simulate this situation somewhat better some runs were done using three acceleration gaps, each with one-third of the

voltage used in the single gap runs. The angle between the gaps was 25° . The result for the 30° phase is plotted as a dashed line in Fig. 9. The blow-up at the beginning of the capture is seen to be a factor two smaller than in the single gap case, but tends to coincide at the end of the capture. This indicates a blow-up factor varying between 1.5 and 4 for the case $\cos \varphi_s = 0.1$.

Corresponding calculations for the case $\cos \varphi_s = 0.3$ yield for the main part of the capture time a factor below 1.5 for φ_o between 0° and 30° , and below 2 for $\varphi_o = 60^\circ$. A substantial drift during the initial acceleration results in a blow-up factor of 2-3 when $\varphi_o = 75^\circ$.

The sensitivity to misalignment of the acceleration gap with respect to the magnetic centre has also been tested. Fig. 10 shows the result of computations where the magnetic centre was displaced 4 mm. The dimension of the final ellipses are the same as in the centred case, but a considerable coherent oscillation is present. Initial centring, Fig. 11, with respect to the magnetic centre resulted also in a coherent oscillation. These results indicate the necessity

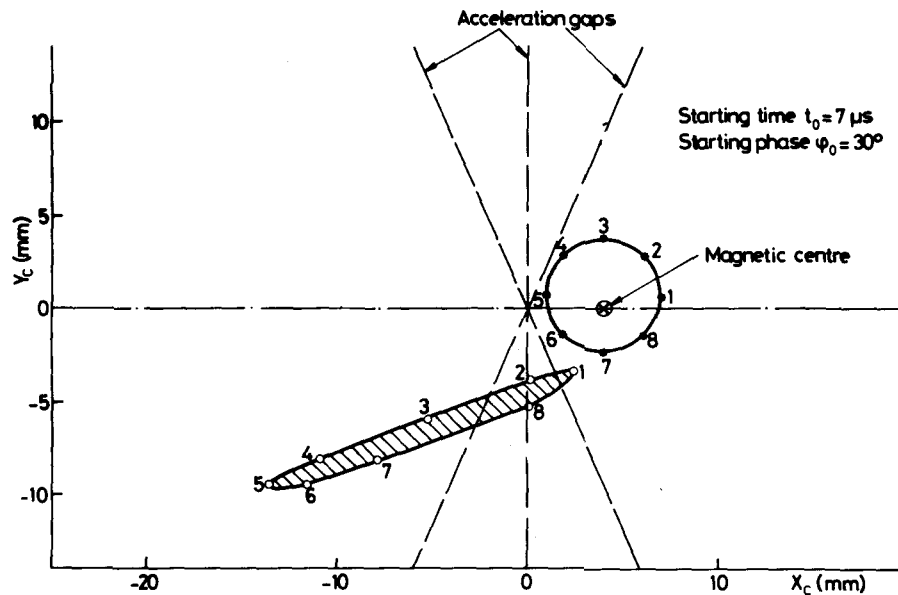


Fig. 11. Distribution of orbit centres after 800 turns when magnetic centre displaced 4 mm. Initial positions marked with stars

of having an accurate knowledge of the position of the magnetic centre or to provide means for adjustments of the acceleration gap in order to find the position giving the smallest amplitudes. It should be mentioned that in the present CERN SC the position of the magnetic centre is known with an accuracy of ~ 1 cm.

The results of radial amplitude measurements with the shadow method¹⁵ in the model cyclotron are summarised in Table 2. The amplitudes are obtained from the total width of the shadow. The tendency of a decrease in amplitude with increased $\cos \varphi_s$ is in good agreement with the calculations. An amplitude build up during the return of the particles towards the centre in the first phase

oscillation explains why bigger amplitudes are found when operating with frequency modulation than with fixed frequency. A reduction of ~30% of these amplitudes was obtained by a realignment of the central geometry.

Table 2. MICRO SC RADIAL AMPLITUDES

df/dt (MHz/ms)	$\cos \varphi_S$	Maximum amplitude (mm)
0.0	(0)	6.8
-5.0	0.055	14.4
-10.0	0.11	11.7
-20.0	0.22	7.0

6. ACKNOWLEDGEMENTS

I would like to express my gratitude to Dr. E. G. Michaelis for his support and encouragement. I am indebted to Dr. Vogt-Nilsen for helpful discussions and for advice in the use of his computer codes. The successful operation of the model cyclotron is largely due to P. Mulder and A. Zanada. I also want to thank R. Giannini for helping me with computations and measurements.

DISCUSSION

Speaker addressed: S. Holm (CERN)

Question by E. G. Auld (UBC): In preparing the model cyclotron for beam tests, how closely was the magnetic field made to match the field of the synchrocyclotron?

Answer: The magnetic field of the model cyclotron matches quite closely the present field of the CERN synchrocyclotron out to a radius of 10-15 cm. We intend to re-shim the synchrocyclotron field to get $K = 2$ a bit further out when we have drilled the hole for the ion-source in the yokes.

REFERENCES

1. Kullander, S., CERN 66-27, (1966).
2. McKenzie, K. R., *Nucl. Instr. Meth.* **31**, 139, (1964).
3. Lawson, J. D., *Nucl. Instr. Meth.* **34**, 173, (1965).
4. Holm, S., *Nucl. Instr. Meth.* **64**, 317, (1968).
5. Kullander, S., CERN M-55, (1966).
6. Scanlon, J. P., Induced Radial Amplitudes in the Modified Cyclotron, private communication, (1966).
7. Blosser, H. G., CERN MSC Internal Report, (1967).
8. Giannini, R. and Susini, A., CERN 68-18, (1968).
9. Mulder, P., MSC/26.1/120, February 1967; MSC/26.1/814, October 1967; MSC/26.1/660, September 1966.
10. Galiana, R. Proceedings of this Conference, p. 728
11. Bohm, D. and Foldy, L. L., *Phys. Rev.* **72**, 649, (1947).
12. Comiti, S. and Giannini, R., MSC Internal Report 68-4, (1967).
13. Kullander, S., *Nucl. Instr. Meth.* **62**, 169, (1968).
14. Mandrillon, P., CERN MSC-69-3.
15. Garren, A. A. and Smith, L., CERN 63-19, 18, (1963).